

Full Duplex Emulation via Spatial Separation of Half Duplex Nodes in a Planar Cellular Network

Henning Thomsen, Dong Min Kim, Petar Popovski, Nuno K. Pratas, Elisabeth de Carvalho

Department of Electronic Systems, Aalborg University, Denmark

Email: {ht, dmk, petarp, nup, edc}@es.aau.dk

Abstract—A Full Duplex Base Station (FD-BS) can be used to serve simultaneously two Half-Duplex (HD) Mobile Stations (MSs), one working in the uplink and one in the downlink, respectively. The same functionality can be realized by having two interconnected and spatially separated Half Duplex Base Stations (HD-BSs), which is a scheme termed *CoMPflex* (CoMP for In-Band Wireless Full Duplex). A FD-BS can be seen as a special case of CoMPflex with separation distance zero. In this paper we study the performance of CoMPflex in a two-dimensional cellular scenario using stochastic geometry and compare it to the one achieved by FD-BSs. By deriving the Cumulative Distribution Functions, we show that CoMPflex brings BSs closer to the MSs they are serving, while increasing the distance between a MS and interfering MSs. Furthermore, the results show that CoMPflex brings benefits over FD-BS in terms of communication reliability. Following the trend of wireless network densification, CoMPflex can be regarded as a method with a great potential to effectively use the dense HD deployments.

Index Terms—Full Duplex, Cellular Communications, Clustering, Network Densification, Spatial Model.

I. INTRODUCTION

As the wireless cellular networks evolve towards the 5G generation, it is expected that the number of Base Stations (BSs) per area will noticeably increase [1], leading to *network densification*. The availability of multiple proximate and interconnected BSs leads to the usage of cooperative transmission/reception techniques, commonly referred to as *Coordinated Multi-Point (CoMP)* [2]. Motivated by these recent trends, a transmission scheme for serving bidirectional traffic simultaneously via spatially separated HD-BSs was investigated in [3]. The scheme emulates Full Duplex (FD) operation using two interconnected HD-BSs, and is termed *CoMPflex*: CoMP for In-Band Wireless Full-Duplex. In the initial work, the performance was analyzed through a simplified one-dimensional Wyner-type deployment model. CoMPflex can be seen as a generalization of FD, where a FD BS corresponds to CoMPflex with interconnection distance zero. We show that the nonzero separation distance in CoMPflex brings two benefits: (i) The distance between a BS and its associated Mobile Stations (MSs) decreases; and (ii) the distance between two interfering MSs increases. This translates into improved transmission success probability in uplink (UL) and downlink (DL).

The use of in-band FD wireless transceivers [4] has recently received significant attention. However, due to the high transceiver complexity, FD is currently only feasible at the network infrastructure side [5] and the MSs keep the HD transceiver mode. An in-band FD BS can serve one UL and

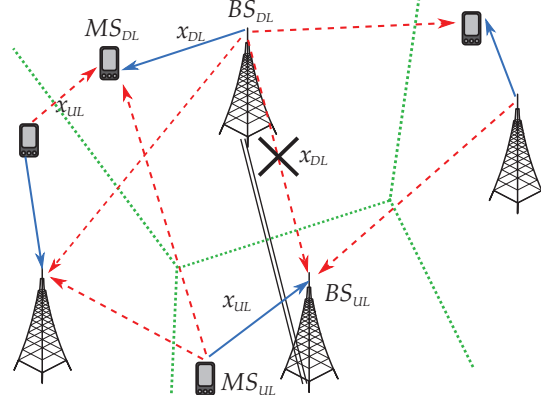


Figure 1: CoMPflex system model.

one DL MSs simultaneously, on the same frequency. Other approaches to FD emulation by HD devices have been studied in the literature, such as having the transmissions in UL and DL (partially) overlap in time. That is, the UL and DL time slots, which conventionally should take place at separate time intervals, are now overlapping, an approach used by the Rapid On-Off Division Duplexing (RODD) in [6]. The authors of [7] consider the physical UL and DL channels themselves, and have them overlap. Compared to these approaches, CoMPflex takes advantage of the spatial dimensions in a cellular network.

In this paper, we treat CoMPflex in a two-dimensional scenario, with planar deployment of interconnected HD-BSs. Following the trend in the literature for modeling spatial randomness of network nodes, we analyze the performance using the tools of stochastic geometry. Stochastic geometry has been used in many papers in the literature to model the placement of network nodes, including FD capable ones as in [8]. The setup of CoMPflex is shown in Fig. 1, where one HD-BS working in the UL cooperates via a wired connection (double solid line) with another HD-BS that operates in the DL. The solid arrows indicate signals; the dashed arrows indicate interference. Two interfering cells are also shown, and the boundaries between them are indicated by dotted lines. Using the interconnection link, the interference from the DL-BS to the UL-BS is perfectly canceled. Note that, for the sake of clarity, not all interference from neighboring cells is shown.

II. SYSTEM MODEL

We consider a scenario where HD-BSs serve HD-MSs with bidirectional traffic. We assume Rayleigh fading with unit mean power. The power of the channel between nodes i and j is written g_{ij} , and from the assumption of Rayleigh fading we

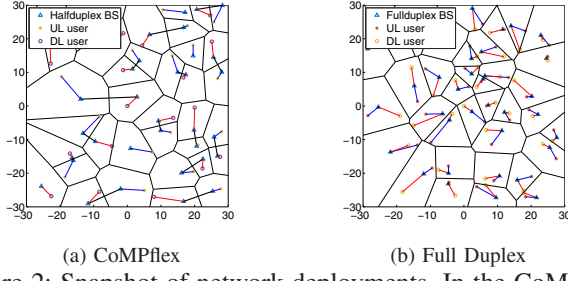


Figure 2: Snapshot of network deployments. In the CoMPflex deployment, each bold line indicates a CoMPflex pair.

have $g_{ij} \sim \text{Exp}(1)$.¹ The distance between nodes i and j is written as r_{ij} . We use the pathloss model $\ell(r) = r^{-\alpha}$, where α is the path loss exponent. We assume Additive White Gaussian Noise (AWGN) with power σ^2 . Full channel state information is assumed at all nodes. The default transmission power of a BS and MS is P_B and P_M , respectively.

A. Deployment Assumptions

We assume that the BSs are deployed according to a Poisson Point Process (PPP) Φ_C with intensity λ_C . The i -th BS located at $\mathbf{x}_i \in \mathbb{R}^2$, defines a *Voronoi region* $\mathcal{V}(\mathbf{x}_i)$,

$$\mathcal{V}(\mathbf{x}_i) = \{\mathbf{x} \in \mathbb{R}^2 \mid \|\mathbf{x} - \mathbf{x}_i\| \leq \|\mathbf{x} - \mathbf{x}_j\|, j \neq i\}, \quad (1)$$

where $\|\cdot\|$ is the Euclidean distance. This region consists of those points \mathbf{x} in \mathbb{R}^2 that are closer to the BS at \mathbf{x}_i than any other BS. From this definition, the intersection of any two Voronoi regions $\mathcal{V}(\mathbf{x}_i)$ and $\mathcal{V}(\mathbf{x}_j)$ is empty, when $i \neq j$. This concept will be important when we consider the MS association in Subsec. II-C. We assume that the Voronoi tessellation determines the rule by which the MS associates with the BS, both for DL and UL, and further that, at a specific time, only one MS randomly located in a Voronoi cell is active.

B. BS Pairing

As stated previously, in CoMPflex we assume that all nodes are HD. We define a *CoMPflex pair* as two adjacent and connected HD-BSs, one serving UL and the other DL traffic. The algorithm for pairing the BSs works as follows:

Given a deployment Φ_C , we consider a finite observation window with dimensions s km (i.e. of size s^2 km²), and choose a BS at random in this window. We then list all the *unpaired* neighbors of this BS, and choose one of those randomly. These two BSs are then considered to be a CoMPflex pair. The algorithm then proceeds to the other unpaired BSs, and pairs the adjacent ones that are unpaired. The BS closest to the origin is called the *typical* BS. Fig. 2a shows one instance of the algorithm, where the CoMPflex pairs are indicated by bold lines between the corresponding BSs (shown as triangles in the figure). In each CoMPflex pair, one BS is assigned either UL or DL randomly with probability 0.5 for each. The other BS is assigned the opposite traffic direction. Given a MS

¹The notation $g \sim \text{Exp}(\mu)$, means that g is exponentially distributed with parameter μ .

i , the BS serving that MS is denoted by $B(i)$. The algorithm terminates when it is no longer possible to pair any BSs. By the rule of pairing, in any CoMPflex pair the two BSs must have adjacent Voronoi regions. Therefore, any BS whose Voronoi region is surrounded by Voronoi regions that belong to paired BSs remains unpaired. We assign the unpaired BSs either as UL or DL at random, with probability 0.5 for each.

After the BS pairing, all BSs have been assigned either UL or DL. Since BSs are assigned either UL or DL at random, on average half of the BSs are UL, the other half, DL. We have $\lambda_C = \lambda_{C,U} + \lambda_{C,D}$, where $\lambda_{C,U}$ is the density of the CoMPflex UL-BSs, and $\lambda_{C,D}$ the density of the CoMPflex DL-BSs.

We recall that given a PPP Φ with intensity λ , we can define a new process by independently selecting each point in Φ with probability p , resulting in a *thinned* PPP Φ' with intensity $p\lambda$. We approximate the point processes of UL-BSs and DL-BSs as independent thinned PPPs. This is only an approximation, as from the algorithm it follows that the selection of DL/UL is not independent, since a DL-BS must be adjacent to a UL-BS.

C. User Association and Scheduling

Given the Voronoi regions defined by the BS deployment, the MS in a given region is scheduled to be served by the BS corresponding to that region. By the definition of a Voronoi region, a MS is associated to one unique BS. More specifically, for every Voronoi region $\mathcal{V}(\mathbf{x}_i)$ one MS is attached to this BS. The position of the MS is chosen uniformly at random in the region. The traffic direction of the MS is matched to the corresponding BS, i.e. if the BS is UL, then the MS has UL traffic, similarly for DL.

A snapshot of the deployment and pairing of BSs, along with the associated UL and DL MSs, is shown in Fig. 2a.

D. Full Duplex Baseline Scheme

In the FD baseline scheme, the BSs are deployed according to a PPP Φ_F with intensity $\lambda_F = 0.5\lambda_C$. In each Voronoi region, one UL MS and one DL MS is served. The location of the two MSs attached to BS i at location \mathbf{x}_i is chosen uniformly at random inside the Voronoi region $\mathcal{V}(\mathbf{x}_i)$ of the BS. The two MSs are assumed to be HD devices. Note that in this setting, the number of MSs is the same as that of CoMPflex, since each FD BS serves two MSs.

III. SIGNAL MODEL

The UL signal to interference plus noise ratio (SINR) at BS $B(i)$ is

$$\gamma_{B(i)} = \frac{g_{i,B(i)} \ell(r_{i,B(i)}) P_M}{I_{B(i)}^\psi + I_{B(i)}^\varphi + \sigma^2}. \quad (2)$$

In the above, the numerator represents the UL signal. In the denominator, the term $I_{B(i)}^\psi$ is the interference from other DL

BSs, $I_{B(i)}^\varphi$ is the interference from other UL MSs, and σ^2 is the AWGN. The interference can be written as:

$$I_{B(i)}^\psi = \sum_{u \in \psi_{B(i)}} g_{u,B(i)} \ell(r_{u,B(i)}) P_B, \quad (3)$$

$$I_{B(i)}^\varphi = \sum_{v \in \varphi_{B(i)}} g_{v,B(i)} \ell(r_{v,B(i)}) P_M, \quad (4)$$

where $\psi_{B(i)}$ and $\varphi_{B(i)}$ are the sets of interfering BSs and MSs respectively. The DL SINR at MS j is given as

$$\gamma_j = \frac{g_{B(j),j} \ell(r_{B(j),j}) P_B}{I_j^\psi + I_j^\varphi + \sigma^2}. \quad (5)$$

In the above, the numerator represents the DL signal. The first term in the denominator, I_j^ψ , is the aggregate interference from other DL BSs to DL MS j , and I_j^φ is the interference from the other UL MSs. The interference terms equal

$$I_j^\psi = \sum_{u \in \psi_j} g_{u,j} \ell(r_{u,j}) P_B, \quad (6)$$

$$I_j^\varphi = \sum_{v \in \varphi_j} g_{v,j} \ell(r_{v,j}) P_M, \quad (7)$$

where ψ_j and φ_j are the sets of interfering BSs and MSs.

IV. RELIABILITY ANALYSIS

We analyze the performance of CoMPflex using the transmission success probability. This metric and its complement, the outage probability, are often used in works that analyze cellular networks through stochastic geometry. In the analysis, we consider a pair of typical BSs and their associated MSs. The typical UL-BS is denoted $B(U)$ and the DL-BS $B(D)$, while the UL-MS and DL-MS are denoted U and D respectively. These BSs and MSs represent the performance of the entire network. We write the SINR at this BS as γ_U (for UL). Similarly, the DL SINR at a typical MS is written as γ_D . A transmission is successful if the SINR is not lower than the target threshold SINR at the receiver.

A. UL and DL Distance Distributions

Recall that the BSs are deployed according to a PPP with density λ_C . The distribution of the distance between a DL-BS $B(i)$ and its associated MS i is denoted $f_{r_{B(i),i}}(r)$. In deriving this distribution, we assume that the BS is located at the origin, i.e. we consider a typical BS. The distance is then denoted $f_{r_{U,B(U)}}(r)$. Similarly, the density of the distance between a MS i and its UL-BS $B(j)$ is written $f_{r_{B(U),U}}(r)$.

As stated from the assumptions, the location of the scheduled MS is uniform at random inside the Voronoi region of the BS. For analytical tractability, we assume that the location of the MS can be any point in \mathbb{R}^2 . Under this assumption, the distance from the typical BS to its MS then has the Cumulative Distribution Function (CDF):

$$F_{r_{B(U),U}}(r) = \Pr\{r_{B(i),i} \leq r\} = 1 - \exp(-\lambda_C \pi r^2), \quad (8)$$

This simplification is routinely made in the literature (see e.g. [9]) for analytical tractability. We assume that the UL distance CDF $F_{r_{U,B(U)}}(r)$ is the same as the DL. The numerical results confirm that this approximation is reasonable.

B. Transmission Success Probability of CoMPflex

In this section, we approximate the success probabilities in UL and DL for CoMPflex. In the derivations, we assume that BSs and MSs are deployed according to independent PPPs with density λ_C . Note that we approximate the locations of the MSs as a PPP, even though they are constrained to be inside the Voronoi cell of their serving BS. Also recall that the interference from the paired DL-BS to the UL-BS is cancelled, and this is reflected in the interference expressions in the proof.

Theorem 1. Assuming independent PPP deployment of MSs and BSs, the success probability in UL in CoMPflex is

$$P_U^C = 2\pi\lambda_C \int_0^\infty r \exp(-\pi\lambda_C r^2 - s\sigma^2) \mathcal{L}_\psi(s) \mathcal{L}_\varphi(s) dr, \quad (9)$$

where $s = \frac{\mu \beta_U r^\alpha}{P_M}$ and the Laplace transforms of the interference from BSs $\mathcal{L}_\psi(s)$ and MSs $\mathcal{L}_\varphi(s)$ are

$$\begin{aligned} \mathcal{L}_\psi(s) &= \int_0^\infty 2\pi\lambda_{C,D} t \exp(-\pi\lambda_{C,D} t^2) \cdot \\ &\exp\left(-2\pi\lambda_{C,D} \int_t^\infty \frac{\beta_U \frac{P_B}{P_M} \left(\frac{r}{x}\right)^\alpha}{1 + \beta_U \frac{P_B}{P_M} \left(\frac{r}{x}\right)^\alpha} x dx\right) dt, \end{aligned} \quad (10)$$

$$\mathcal{L}_\varphi(s) = \exp\left(-2\pi\lambda_{C,U} \int_r^\infty \frac{\beta_U \left(\frac{r}{y}\right)^\alpha}{1 + \beta_U \left(\frac{r}{y}\right)^\alpha} y dy\right). \quad (11)$$

Proof. We consider the UL SINR γ_U , and choose a typical BS. Then we condition on the distance from the BS to the nearest UL-MS being r . The success probability is

$$P_U^C = \Pr\{\gamma_U \geq \beta_U\} = \int_0^\infty \Pr\{\gamma_U \geq \beta_U | r\} f_{r_{U,B(U)}}(r) dr.$$

The conditioned CDF of the SINR equals (note that we drop the explicit notation of the conditioning for readability)

$$\begin{aligned} \Pr\{\gamma_U \geq \beta_U | r\} &= \Pr\left\{\frac{g_{U,B(U)} r^{-\alpha} P_M}{I_{B(U)}^\psi + I_{B(U)}^\varphi + \sigma^2} \geq \beta_U\right\} \\ &\stackrel{(a)}{=} \mathbb{E}\left[\exp\left(-s(I_{B(U)}^\psi + I_{B(U)}^\varphi + \sigma^2)\right)\right] \\ &= \exp(-s\sigma^2) \mathcal{L}_\psi(s) \mathcal{L}_\varphi(s), \end{aligned}$$

where in (a) we have used that $g_{U,B(U)} \sim \text{Exp}(\mu)$, and we set $s = \frac{\mu \beta_U r^\alpha}{P_M}$. We now derive the interference from the other DL-BSs. In the derivation, we condition on the distance to the nearest interfering DL-BS to be t because this distance is independent from r . The distance t represents the approximation of the distance to the paired DL-BS, whose

transmission is perfectly cancelled and this gives an upper bound. The density of interfering DL-BSSs is $\lambda_{C,D}$. Then

$$\begin{aligned}\mathcal{L}_\psi(s) &= \mathbb{E}_{I^\psi} \left[\exp \left(-s \sum_{i \in \psi_B(i)} P_B g_{i,B(i)} r_{i,B(i)}^{-\alpha} \right) \right] \\ &\stackrel{(a)}{=} \mathbb{E}_{I^\psi} \left[\prod_{i \in \psi_B(i)} \mathbb{E}_g \left[\exp \left(-s P_B g_{i,B(i)} r_{i,B(i)}^{-\alpha} \right) \right] \right] \\ &\stackrel{(b)}{=} \exp \left(-2\pi\lambda_{C,D} \int_t^\infty (1 - \mathbb{E}_g [\exp(-s P_B g_{i,B(i)} x^{-\alpha})]) dx \right) \\ &\stackrel{(c)}{=} \exp \left(-2\pi\lambda_{C,D} \int_t^\infty \left(\frac{s P_B x^{-\alpha}}{1 + s P_B x^{-\alpha}} \right) dx \right),\end{aligned}$$

where in (a) we have used that the channels $g_{i,B(i)}$ are independent, (b) is from the Probability Generating Functional (PGFL) of a PPP with density $\lambda_{C,D}$ and $x = r_{i,B(i)}$, and in (c) we rewrite using the Moment Generating Function (MGF) of an exponential random variable. Combining this with the Probability Density Function (PDF) of the distance t and using $s = \frac{\mu\beta_U r^\alpha}{P_M}$, we get Eq. (10). Using similar arguments, Eq. (11) also can be derived. Note however, that in Eq. (11), the distance to the nearest interfering UL-MS follows the same distribution as the distance to the served UL-MS. \square

For DL, recall that we approximate the interfering MSs as a PPP, and this approximation implies that an interfering UL-MS could be inside the Voronoi cell of the DL-MS. However, in CoMPflex there is exactly one MS in each cell. Therefore, the interference is overestimated.

Theorem 2. Assuming independent PPP deployment of MSs and BSs, the success probability in DL for CoMPflex is

$$P_D^C = 2\pi\lambda_C \int_0^\infty r \exp(-\pi\lambda_C r^2 - s\sigma^2) \mathcal{L}_\psi(s) \mathcal{L}_\varphi(s) dr, \quad (12)$$

where $s = \frac{\mu\beta_D r^\alpha}{P_B}$ and the Laplace transforms of the interference from BSs $\mathcal{L}_\psi(s)$ and MSs $\mathcal{L}_\varphi(s)$ are

$$\mathcal{L}_\psi(s) = \exp \left(-2\pi\lambda_{C,D} \int_r^\infty \frac{\beta_D \left(\frac{r}{x}\right)^\alpha}{1 + \beta_D \left(\frac{r}{x}\right)^\alpha} x dx \right), \quad (13)$$

$$\mathcal{L}_\varphi(s) = \exp \left(-2\pi\lambda_{C,U} \int_0^\infty \frac{\beta_D \frac{P_M}{P_B} \left(\frac{r}{y}\right)^\alpha}{1 + \beta_D \frac{P_M}{P_B} \left(\frac{r}{y}\right)^\alpha} y dy \right). \quad (14)$$

Proof. The proof follows similar steps as the one for UL, and so is omitted to avoid duplication. \square

Note that the integration range of Eq. (14) starts at 0, since there is no interference cancellation in DL, contrary to UL. From this, we obtain a lower bound on the success probability.

C. Transmission Success Probability of Full Duplex

In the FD baseline, for DL, Eq. (9) in [10] gives the outage probability of a scenario similar to our FD baseline. The success probability can be directly derived from that equation.

In deriving the UL success probability, we can use a strategy similar to the one used for DL in [10]. Then, the UL success probability in the FD baseline is

$$P_U^F = 2\pi\lambda_F \int_0^\infty r \exp(-\pi\lambda_F r^2 - s\sigma^2) \mathcal{L}_\psi(s) \mathcal{L}_\varphi(s) dr, \quad (15)$$

where $s = \frac{\mu\beta_U r^\alpha}{P_M}$ and the Laplace transforms of the interference from BSs $\mathcal{L}_\psi(s)$ and MSs $\mathcal{L}_\varphi(s)$ are

$$\mathcal{L}_\psi(s) = \exp \left(-2\pi\lambda_F \int_r^\infty \frac{\beta_U \frac{P_B}{P_M} \left(\frac{r}{x}\right)^\alpha}{1 + \beta_U \frac{P_B}{P_M} \left(\frac{r}{x}\right)^\alpha} x dx \right), \quad (16)$$

$$\mathcal{L}_\varphi(s) = \exp \left(-2\pi\lambda_F \int_r^\infty \frac{\beta_U \left(\frac{r}{y}\right)^\alpha}{1 + \beta_U \left(\frac{r}{y}\right)^\alpha} y dy \right). \quad (17)$$

V. NUMERICAL RESULTS

We show the performance of CoMPflex, and the comparison with the FD baseline schemes, using both numerical simulations and the analytical model given in the previous section. The simulation assumptions are shown in Table I, where the densities are chosen comparable with [10].

Table I: Simulation parameters.

Parameter	Description	Simulation Setting
s	Size of observation window	200 km
λ_C	BS density (CoMPflex)	0.02 BS/km ²
λ_F	BS density (FD)	0.01 BS/km ²
σ^2	Noise power at MS and BS	-174 dBm
α	Path loss exponent	4
β	SINR thresholds	-20, -15, -10, ..., 20 dB
P_B	BS transmission power	40 dBm
P_M	MS transmission power	20 dBm

We study the success probability in both UL and DL for CoMPflex, in terms of varying the SINR threshold, and compare with FD. The BS and MS transmission powers are held constant according to the values in Tab. I. The UL success probability for CoMPflex and FD, both simulation and analytical, is shown in Fig. 3. Here, the analytical curve approximates the simulated values quite closely. However, the success probability in UL is lower than DL, which can be partially explained by the MS power being lower than the BS power.

The resulting success probability for DL is shown in Fig. 4. In this figure, we can observe that the analytical derivations result in a lower bound on the success probability. This was to be expected, since the point processes in CoMPflex are not truly PPP. However, as the figure shows, the PPP approximation is quite close and serves well as an indicator of the expected performance of CoMPflex. We also observe that the success probability in CoMPflex is about 30% higher than FD, for most of the range of SINR thresholds. The explanation of this can be attributed to how CoMPflex affects the distances of the signal and interference links.

Since one of the main features in CoMPflex is that it brings the MSs closer to the serving BSs, we analyze and compare the CDFs of the various distances for signal and intra-cell interference links in CoMPflex and FD. This comparison is

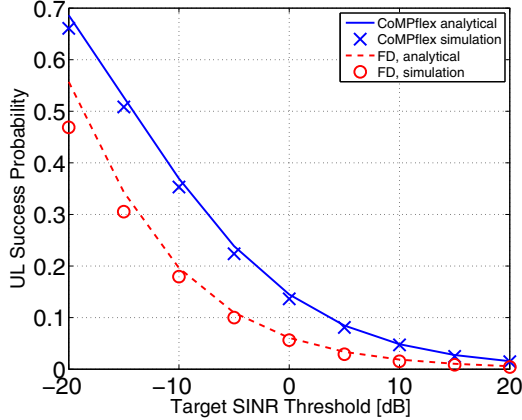


Figure 3: Success Probability in UL vs. SINR threshold.

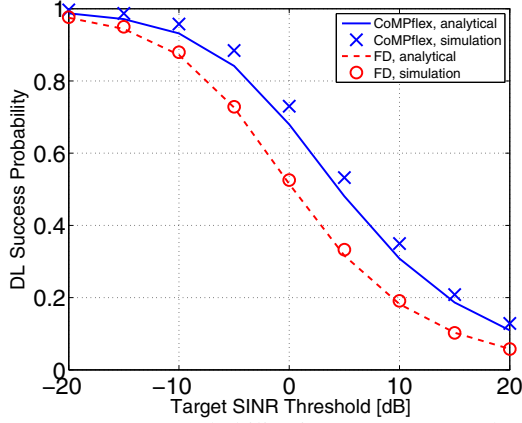


Figure 4: Success Probability in DL vs. SINR threshold.

shown in Fig. 5. The simulated CDF are shown as lines, while the analytical CDF using Eq. (8) are shown as markers². From this figure, we can observe two important points:

First, we compare the CDFs of the distances between an UL-MS and BS, and between a BS and DL-MS. We see that for both CoMPflex and FD, the UL and DL distance curves overlap. This implies that the distances of UL and DL follow the same distribution. What is also interesting is that the CDFs of the distances in CoMPflex are shifted to the *left*, compared to FD. This means that the lower MS to BS distances have higher probability in CoMPflex compared to FD.

Second, the CDF curve of the intra-cell interference distance in CoMPflex is shifted to the *right* compared to FD. This means that higher interference distances have higher probability in CoMPflex compared to FD. Taken together, these two points can explain the performance advantages of CoMPflex over FD, which come from having a lower signal distance and a higher interference distance *simultaneously*.

VI. CONCLUSION

In this work, we have analyzed the performance of CoMPflex in a planar network setting, and compared it with a FD baseline scheme. We have derived the success probability

²Note that the analytical CDF of CoMPflex is shifted to the left, compared to FD, since $\lambda_F = 0.5\lambda_C$

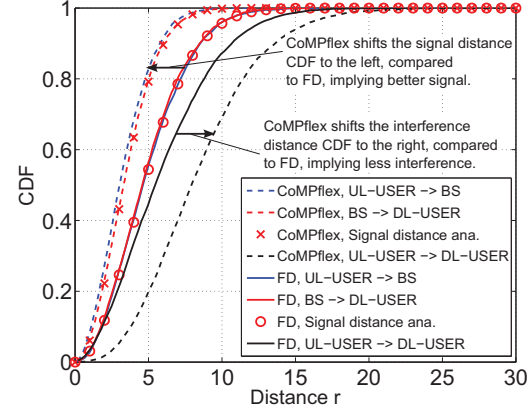


Figure 5: Comparison of the CDFs of the node distances in the CoMPflex and FD scenarios.

for UL and DL, and validated the results via simulations. It was observed that the success probability of both UL and DL was higher for CoMPflex than in FD, an effect which can be attributed to the effects of CoMPflex on the node distances. Thus it is beneficial to consider the usage of HD devices instead of FD, which is also useful for using already existing technology and avoiding the signal complexities of FD.

One promising research direction is to consider more than two connected BSs, and more general clustering criteria. Also, it would be interesting to compare CoMPflex with other interference mitigation techniques such as CoMP.

ACKNOWLEDGMENT

This work was supported by Innovation Fund Denmark, via the Virtuoso project.

REFERENCES

- [1] F. Boccardi, R. W. Heath Jr, A. Lozano, T. L. Marzetta, and P. Popovski, “Five Disruptive Technology Directions for 5G,” *IEEE Commun. Mag.*, vol. 52, pp. 74–80, Feb. 2014.
- [2] D. Lee, H. Seo, B. Clerckx, E. Hardouin, D. Mazzarese, S. Nagata, and K. Sayana, “Coordinated Multipoint Transmission and Reception in LTE-Advanced: Deployment Scenarios and Operational Challenges,” *IEEE Commun. Mag.*, vol. 50, pp. 148–155, Feb. 2012.
- [3] H. Thomsen, P. Popovski, E. De Carvalho, N. Pratas, D. Kim, and F. Boccardi, “CoMPflex: CoMP for In-Band Wireless Full Duplex,” *IEEE Wirel. Commun. Lett.*, vol. 5, no. 2, pp. 144–147, 2016.
- [4] A. Sabharwal, P. Schniter, D. Guo, D. Bliss, S. Rangarajan, and R. Wichman, “In-Band Full-Duplex Wireless: Challenges and Opportunities,” *IEEE J. Select. Areas Commun.*, vol. 32, pp. 1637–1652, Sept. 2014.
- [5] E. Dahlman, G. Mildh, S. Parkvall, J. Peisa, J. Sachs, Y. Selen, and J. Skold, “5G Wireless Access: Requirements and Realization,” *IEEE Commun. Mag.*, vol. 52, pp. 42–47, Dec. 2014.
- [6] D. Guo and L. Zhang, “Virtual Full-Duplex Wireless Communication via Rapid On-Off-Division Duplex,” in *Proc. Allerton*, Sept. 2010.
- [7] A. AlAmmouri, H. ElSawy, and M.-S. Alouini, “Harvesting Full-Duplex Rate Gains in Cellular Networks with Half-Duplex User Terminals,” in *Proc. IEEE ICC*, May 2016.
- [8] Z. Tong and M. Haenggi, “Throughput Analysis for Full-Duplex Wireless Networks With Imperfect Self-Interference Cancellation,” *IEEE Trans. Commun.*, vol. 63, no. 11, pp. 4490–4500, 2015.
- [9] T. D. Novlan, H. S. Dhillon, and J. G. Andrews, “Analytical Modeling of Uplink Cellular Networks,” *IEEE Trans. Wirel. Commun.*, vol. 12, pp. 2669–2679, Jun. 2013.
- [10] C. Psomas and I. Krikidis, “Outage Analysis of Full-Duplex Architectures in Cellular Networks,” in *Proc. IEEE VTC Spring*, pp. 1–5, 2015.